Enhanced selectivity for Mg^{2+} with a phosphinate-based chelate: APDAP versus APTRA

Edward R. H. Walter, Mark A. Fox, David Parker* and J. A. Gareth Williams*

Department of Chemistry, Durham University, Durham, DH1 3LE U.K.
* E-mail: david.parker@durham.ac.uk   j.a.g.williams@durham.ac.uk

Abstract

o-Aminophenol-N,N,O-triacetate, known as APTRA, is one of the most well-established ligands for targeting magnesium ions but, like other aminocarboxylate ligands, it binds Ca^{2+} much more strongly than Mg^{2+}. The synthesis of an O-phosphinate analogue of APTRA is reported here, namely o-aminophenol-N,N-diacetate-O-phosphinate, referred to as APDAP. Metal binding studies monitored using UV-visible spectroscopy show that the affinity of APDAP for Ca^{2+} is reduced by over two orders of magnitude compared to APTRA, and for Zn^{2+} by over three orders of magnitude, whereas the affinity for Mg^{2+} is attenuated to a much lesser extent, by a factor of only about 7. The selectivity towards Mg^{2+} is thus substantially improved. DFT calculations support the notion that longer P–O and P–C bonds in APDAP (compared to corresponding C–O and C–C bonds in APTRA) favour a larger angle at the metal, an effect that is less unfavourable for smaller ions like Mg^{2+} than for larger ions such as Ca^{2+}. Derivatives of APDAP can be anticipated that will offer improved sensing of Mg^{2+} in the physiologically important millimolar concentration range, in the presence of Ca^{2+}.

Introduction

Amino carboxylates are pre-eminent amongst ligands used to bind to divalent Group 2 metals and hard transition metal ions such as Fe^{3+} and Mn^{2+}.[1,2] EDTA is produced on a huge scale for sequestration and regulation of metal ions in consumer products and inhibition of bacterial growth.[3] Related aminophenolate-based ligands such as BAPTA {1,2-bis(O-aminophenoxy)-ethane-N,N,N',N'-tetra-acetate, Figure 1} were developed in the 1980s by Tsien for the selective binding of Ca^{2+}: the octadenticity favours coordination of the large Ca^{2+} ion.[4] A number of fluorescent analogues of BAPTA were introduced through the incorporation of a fluorescent aromatic in place of, or attached to, one of the aminophenol units (*e.g.*, Fura-2 and Indo-1).[5,6,7] In conjunction with fluorescent microscopy, they have been successfully used for the real-time monitoring of Ca^{2+} concentrations in cell biology, physiology and neurology.[8]
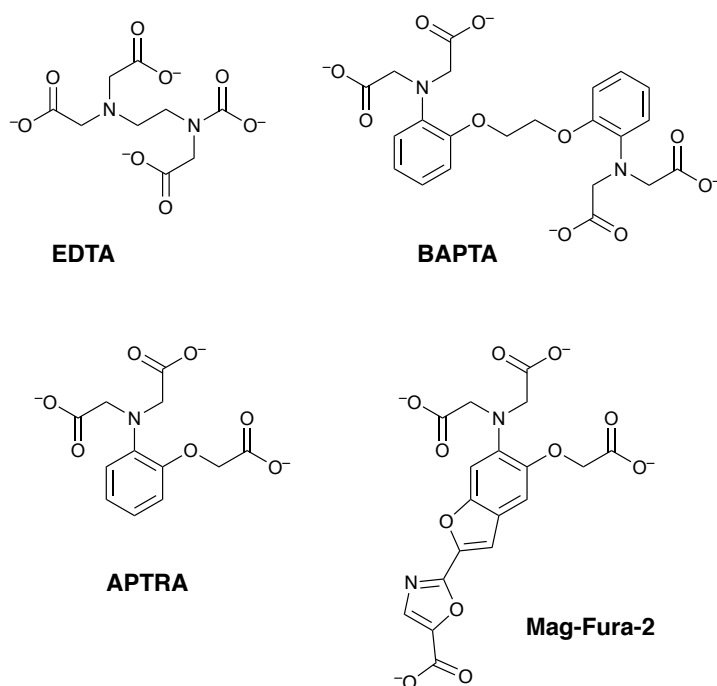

Figure 1 *The structures of selected amino carboxylate ligands: the ubiquitous broad-spectrum ligand EDTA, the Ca^{2+}-selective ligand BAPTA, the APTRA ligand for Mg^{2+} binding, and Mag-Fura-2, a fluorescent derivative of APTRA.*

The smaller Mg^{2+} ion, on the other hand, has seen far less attention – and much less success in terms of efforts to design ligands that bind it with high selectivity. Perhaps the most well-known examples to date are based on the APTRA structure (APTRA = *o*-aminophenol-N,N,O-triacetate,

Figure 1) introduced by London and co-workers in the late 1980s.[9] APTRA is a lower-denticity cousin of BAPTA – potentially pentadentate rather than octadentate – and features three as opposed to two carboxylates per aminophenol unit. Available fluorescent indicators marketed for Mg^{2+} are typically based on the APTRA unit connected to, or incorporating, a fluorescent aromatic reporter group, *e.g.*, Mag-Fura-2 (Figure 1) and related derivatives.[6,10]

Yet, such ligands are not selective for Mg^{2+}. Although their affinity for Ca^{2+} is reduced compared to BAPTA, they still retain a higher affinity for Ca^{2+} than for Mg^{2+} (micromolar versus millimolar) and indeed can be employed as Ca^{2+} indicators to respond over higher concentration ranges than the standard Ca^{2+} probes. Such selectivity issues apply equally to more recently described APTRA-based systems designed to offer longer-wavelength excitation and emission.[11] Meanwhile, the use of bidentate β-keto acids, a quite different strategy explored for Mg^{2+} binding,[12,13] suffers from other limitations, notably the fact that the low denticity favours the formation of mixed ligand species *in vivo*, in which the coordination sphere of the metal ion may be completed by endogenous molecules such as ATP.[14]

Nevertheless, Mg^{2+} remains a highly interesting target bio-medically.[15] It is the second most abundant divalent cation in cells,[16] it plays a key role in the stabilisation of DNA structure,[17] and it is implicated in hundreds of enzymatic reactions.[18] A number of cardiovascular,[19] neurodegenerative[20] and renal[21] diseases have associated with them a mis-regulation of Mg^{2+} concentrations. Greater effort is clearly required on the development of new classes of chelate ligand for selective binding of Mg^{2+}, that can be used in the presence of competitor ions such as Ca^{2+} and Zn^{2+}, yet function in the physiologically important millimolar range: the concentration of "free" Mg^{2+} is thought to be around 1 mM in the majority of mammalian cells.

Results and Discussion

(i) Strategy

Here we describe the synthesis and metal binding properties of a new ligand for Mg^{2+}, namely *o*-aminophenol-N,N-diacetate-O-methylphosphinate, which shall be referred to as APDAP. The APDAP ligand is structurally similar to APTRA, but features a phosphinate group, $-OCH_2P(Me)O_2^-$, in place of the phenolate-bound carboxylate group, $-OCH_2CO_2^-$ (Figure 2). In the binding of divalent metal ions, pentadenticity can thus be maintained with formation of four 5-membered chelate rings, but it was anticipated that the change from a C–O to a P–O bond within one of the chelate rings would serve to reduce the affinity for Ca^{2+} and thus enhance selectivity for Mg^{2+} over Ca^{2+}. The hypothesis has been borne out by the data described below.
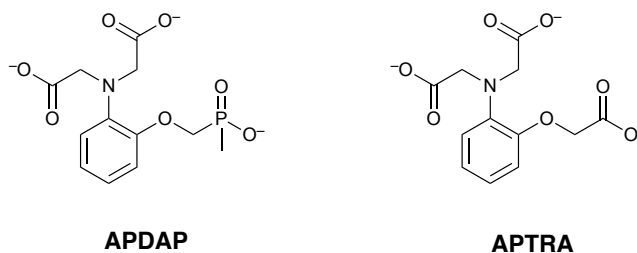

APDAP **APTRA**

Figure 2 *The structure of the new phosphinate ligand **APDAP** shown alongside the tricarboxylate **APTRA**.*

(ii) Synthesis

The synthesis of APDAP was achieved using the two sequences of reactions shown in Scheme 1. The first sequence was used to prepare the phosphinate-containing alkylating agent **4**. Hydrolysis of diethyl methylphosphinate **1** with one equivalent of water led to ethyl methylphosphinate **2**. Condensation of **2** with paraformaldehyde gave alcohol **3**, which was subsequently converted to its mesylate ester **4** in quantitative yield, upon treatment with mesyl chloride in the presence of triethylamine as a base. Owing to the greater nucleophilicity of amines compared to phenols, O-alkylation of *o*-aminophenol would require prior protection of the amine. We chose instead to start from *o*-nitrophenol, **5**, which was O-alkylated using **4** under basic conditions to give **6**; completion of the reaction was visually evident from the loss of

the bright orange colour associated with the 2-nitrophenoxide ion. Following chromatographic purification, reduction of the nitro group using hydrogen gas, catalysed by palladium on carbon, gave the O-alkylated aniline **7**, which was then bis-N-alkylated using ethyl bromoacetate in the presence of base and catalytic NaI, leading to **8** over a period of 4 days. Finally, hydrolysis of the two carboxylate esters and the phosphinate ester of **8** was accomplished using sodium deuteroxide in deuterated methanol / water mixture to give APDAP. The use of deuterated conditions allows the progress of hydrolysis to be readily monitored by ^{1}H and ^{31}P NMR spectroscopy: the ^{31}P resonance shifts from 48.3 to 36.5 ppm on hydrolysis. The purity of the final product was assessed by analytical HPLC using acetonitrile / ammonium bicarbonate as the eluent.

(a)

(b)
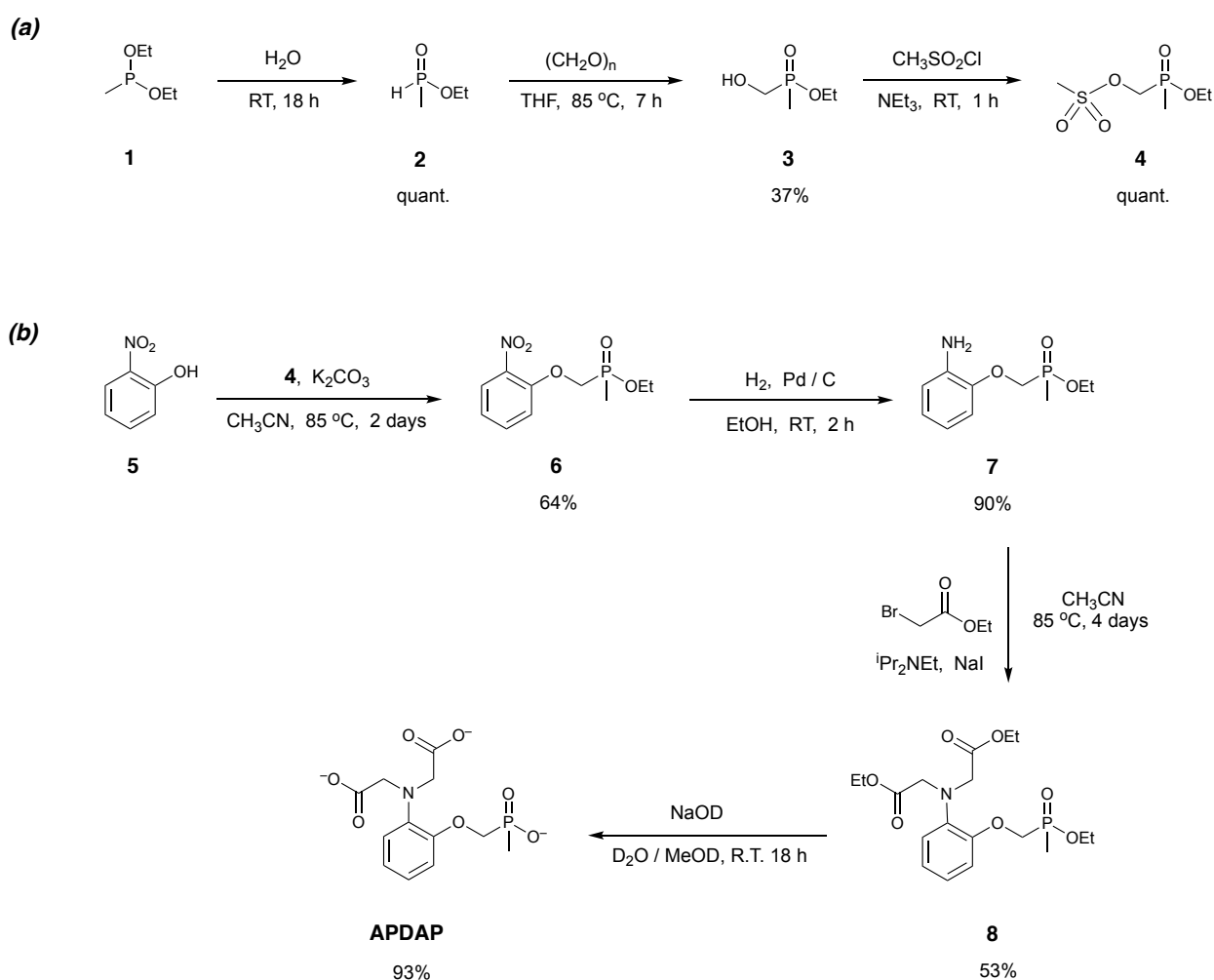
Scheme 1 *Synthesis of (a) the alkylating agent **4** and (b) APDAP from o-nitrophenol*

(iii) Absorption spectroscopy: effect of pH

We employed UV absorption spectroscopy as the method for assessing the metal-binding properties of the new APDAP ligand, which allows a direct comparison to be made with studies of APTRA.[22] Evidently, fluorescence spectroscopy offers greater sensitivity and diversity of applications, but APDAP itself – like APTRA – is only weakly fluorescent and would require short-wavelength excitation that is impracticable for most applications. The conjugation of the APDAP ligand to a fluorescent reporter unit can readily be envisaged to prepare fluorescent derivatives.

The absorption spectrum of APDAP in aqueous solution at pH = 8.5 shows one main band centred at 254 nm (ε = 4480 M^{-1} cm^{-1}) accompanied by a distinct shoulder at 285 nm. The variation of the spectrum with pH was monitored over the pH range 4.5 – 8.5. Acidification leads to a decrease in the absorbance across all wavelengths, particularly the main band at 254 nm: the spectrum under acidic conditions features a broad band with a rather ill-defined maximum around 260 nm (Figure 3). Such changes are consistent with those expected upon protonation of the formerly electron-donating amino group. The sigmoidal fit of the absorbance at 254 nm against pH gave a ground-state pK_a of 6.03(8) (Figure 3, inset). This suggests that, over the normal physiological pH range (pH 6.5 – 7.5), the amine will be largely unprotonated and therefore available for metal ion binding, together with the less basic carboxylates and phosphinate. It is encouraging that there is little change in the absorbance with pH over the above physiological range: metal ion probes that are targeted for use in biomedical areas should ideally not be affected by pH under the prevailing conditions, otherwise an observed response cannot be unequivocally attributed to metal ion binding but rather may arise from variation in pH. Similarly, competitive protonation leading to decomplexation of the target metal ion once bound needs to be avoided. A Mg^{2+}-saturated solution of APDAP showed very little variation with pH in its UV-visible spectrum (Figure 3, inset).

In the case of APTRA, the pK_a has not been accurately determined in the majority of its derivatives, owing to it being somewhat unstable in solution through decarboxylation and oxidation reactions;[23] a pK_a value of 5.5 was determined for one APTRA derivative by absorption spectroscopy.[24] Magnesium-bound APTRA has similarly been found to be largely pH-insensitive.
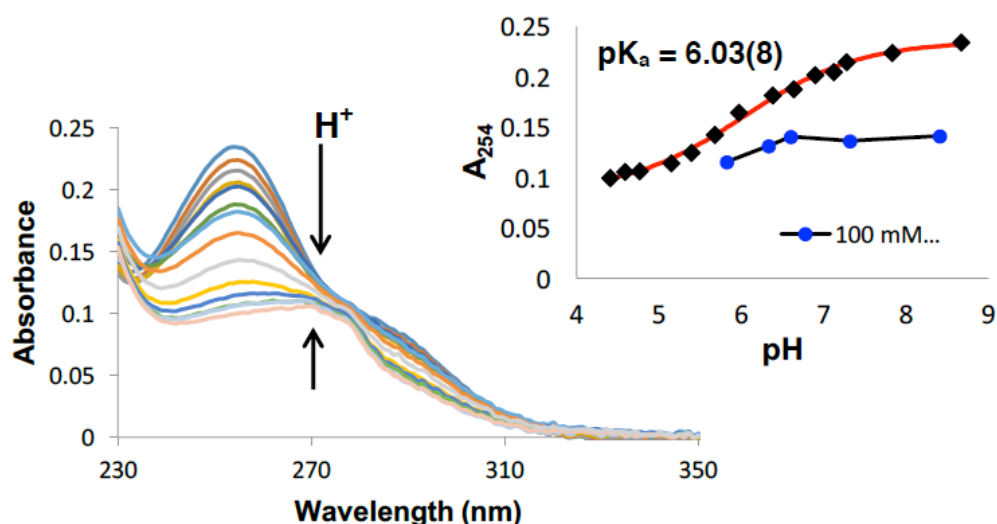

Figure 3 Absorption spectrum of APDAP in aqueous solution at varying pH values between 8.5 and 4.5; concentration = 50 μM, in the presence of 100 mM KCl, T = 298 ± 3 K. The inset shows the sigmoidal fit (red line) to the absorbance at 254 nm against pH (black diamond data points). The blue circles in the inset show the change in the absorption at 254 nm with pH after saturation with Mg^{2+} (100 mM), with a trendline in black.

(iii) Absorption spectroscopy: effect of divalent metal ions Mg^{2+}, Ca^{2+} and Zn^{2+}

The effect of increasing concentrations of the above metal ions on the absorption spectrum was investigated in aqueous solution, buffered to pH = 7.21 using HEPES, at a temperature of 298 ± 1 K. The evolution of the spectra, together with the corresponding fits to estimate binding constants, are shown in Figure 4. The standard deviations indicated were obtained from three independent sets of measurements in each case. The binding affinities of APDAP for each metal ion are compared with those previously reported for APTRA in Table 1.
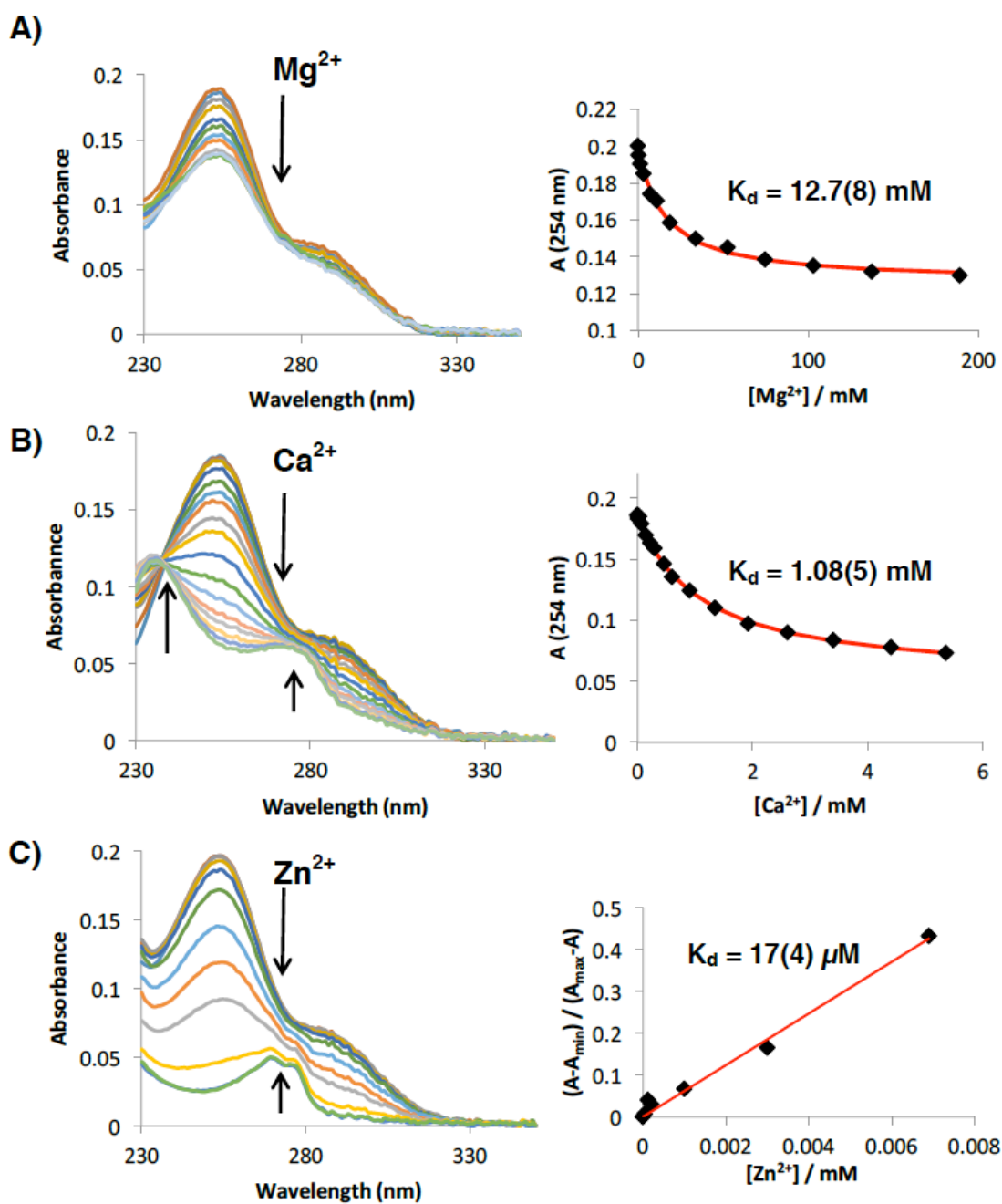
Figure 4 *Absorption spectra (left) and binding curves with associated fits in red (right) for the addition of **(A)** Mg^{2+}, **(B)** Ca^{2+}, and **(C)** Zn^{2+} to APDAP in aqueous solution. The metal chloride salts were used in each case; [APDAP] = 50 μM, [HEPES] = 50 mM, [KCl] = 100 mM, pH = 7.21, T = 298 ± 3 K. The reported binding constants are an average from three separate metal ion titrations, with the standard deviation in parenthesis.*

Table 1 *Comparison of the metal binding affinities of APDAP and APTRA[a, b], obtained via absorption spectroscopy in aqueous solution.*

	APDAP	APTRA
pK_a	6.03(8)	5.5
$K (Mg^{2+}) / M^{-1}$	79(5)	560(30)
$K_d (Mg^{2+})$	12.7(8) mM	1.79 mM
$K (Ca^{2+}) / M^{-1}$	$9.30(5) \times 10^2$	$1.02(7) \times 10^5$
$K_d (Ca^{2+})$	1.08(5) mM	9.80 μM
$K (Zn^{2+}) / M^{-1}$	$6(1) \times 10^4$	$7(1) \times 10^7$
$K_d (Zn^{2+})$	17(4) μM	14 nM

(a) pK_a value of APTRA is from reference 24.
(b) Metal-binding data for APTRA are those of Buccella and co-workers, ref. 22.

For each of the three metal ions investigated, it can be seen that the absorbance of the main bands progressively decreased with increasing concentration of the metal. However, the change in the spectral profile is rather different. In the case of Ca^{2+} and Zn^{2+}, there is a large decrease in absorbance of the main band at 254 nm and of the long-wavelength shoulder, whilst a new band starts to emerge at about 273 nm (with an additional high-energy band at about 237 nm for Ca^{2+}). In contrast, the spectral profile does not change substantially upon addition of Mg^{2+}. The changes with Ca^{2+} and Zn^{2+} are more similar to the effect of protonation (Figure 3) than those induced by Mg^{2+}. One may tentatively conclude, therefore, that the amine plays a less significant role in the binding of Mg^{2+} than Ca^{2+} or Zn^{2+}: it is possible that the APDAP binds Mg^{2+} in a *quasi*-tetradentate O_4 coordination mode, without much participation of the nitrogen lone pair, but for the larger Ca^{2+} ion and for the more polarisable Zn^{2+} ion it is pentadentate O_4N (Figure 5).
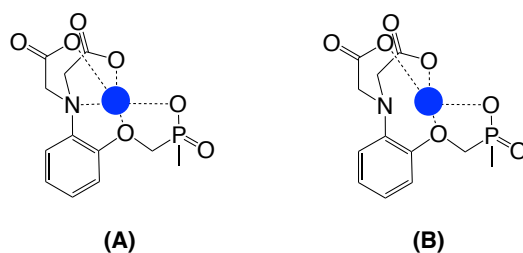
Figure 5 *Plausible coordination modes for APDAP with divalent metal ions: the tetradentate mode (B) may be closer to that adopted by Mg^{2+}, with the pentadentate (A) for Ca^{2+} and Zn^{2+}.*

Inspection of the binding constant data in Table 1 reveals some intriguing differences between APDAP and APTRA. The binding constant of APDAP for Mg^{2+} is 79(5) M^{-1} which is reduced by a factor of approximately 7 compared to that of APTRA.[22] In contrast, the affinity for Ca^{2+} is lowered by a factor of 110. Similarly, the affinity for Zn^{2+} ions plummets by a factor of $> 10^3$. Clearly, then, the selectivity for Ca^{2+} or Zn^{2+} over Mg^{2+} is reduced on going from *O*-carboxylate to the *O*-phosphinate, as desired. Although the new ligand does not show the required selectivity profile for Mg^{2+}, competition from Ca^{2+} and Zn^{2+} will clearly be lowered. Pentadentate ligands showing sensitivity in the millimolar range for both Mg^{2+} *and* Ca^{2+} have not previously been reported. The bidentate β-keto acids mentioned earlier do show such a range, but do not offer the high denticities necessary to avoid formation of mixed ligand species.

(iv) APDAP versus APTRA: a theoretical evaluation

For possible insight into the differing effects of the change from carboxylate to phosphinate on Ca^{2+} and Mg^{2+} binding, a series of DFT calculations was carried out for complexes of the two ligands. Details of the functionals and basis sets employed are given in the Experimental Section. Crystal structures of the Mg^{2+} and Zn^{2+} complexes of APTRA have been reported by Buccella and co-workers, in which the metal ions are *O*$_4$*N*-coordinated by the pentadentate ligand, with the sixth coordination site occupied by a bridging carboxylate from a neighbouring complex.[22] For simplicity in the calculations, and as a more likely parallel of behaviour in solution, the DFT calculations were run with a water molecule occupying the sixth site. The

optimised structures obtained in this way for the Mg^{2+}, Ca^{2+} and Zn^{2+} complexes are shown in Figure S1 of the Supporting Information. There is a good agreement between the calculated M–L bond lengths and those determined crystallographically by Buccella and co-workers for the Mg^{2+} and Zn^{2+} complexes of APTRA (a comparison is provided in Table S1). This offers confidence in the approach, in the absence of crystal structures of the APDAP complexes. Ideally, the calculation of relative metal binding energies would be helpful, but such a task is hampered by the likely increase in coordination number of Ca^{2+} beyond 6, probably up to 8, through coordination of additional water molecules. Multiple anions of the form $[Ca(APTRA)(H_2O)_n]^-$ are likely in solution. We focused instead on differences in key bond lengths and angles in the structures of the Mg^{2+} compared to the Zn^{2+} complexes, which are both expected to be 6-coordinate and which feature metal ions of very similar ionic radius.

From the calculated bond lengths collated in Table 2, it can be seen that, for APTRA, the M–L bond lengths are very similar for the Mg^{2+} and Zn^{2+} complexes. In contrast, for APDAP, there are significant differences between the Mg^{2+} and Zn^{2+} complexes for most of the M–L bonds. In general, M–L bond lengths are shorter in $[Mg(APDAP)(H_2O)]^-$ compared to $[Mg(APTRA)(H_2O)]^-$. Comparing $[Zn(APTRA)(H_2O)]^-$ and $[Zn(APDAP)(H_2O)]^-$, on the other hand, shows little difference between them in M–L bond lengths. The Mg–L lengths are mostly shorter than corresponding Zn–L lengths, for both APTRA and APDAP. The shorter Mg–N compared to Zn–N bond length that is calculated may appear somewhat inconsistent with the conclusions from UV-visible spectroscopy, summarised in Figure 5, that suggest a stronger interaction of the nitrogen lone pair with Zn^{2+} than with Mg^{2+}. However, the UV-visible data are obtained in aqueous solution, where an H_2O molecule or an OH could occupy the sixth coordination site in place of the amine nitrogen atom. The DFT calculations do not allow for this possibility, being based on the solid-state structure. Some caution must therefore be exercised in using the theoretical data, with regard to the spectroscopic changes.

Table 3 summarises the bite angles around the metal for the four complexes. Here again, it is evident that [Mg(APDAP)(H$_2$O)]$^-$ differs from the other three: the bite angles are largest for this complex. Such a trend is consistent with longer P–C and P–O bonds compared to corresponding C–C and C–O bonds (Table S2), but the effect is clearly more significant for the Mg^{2+} complex than for the Zn^{2+} complex (*e.g.*, ArO–M–O angles of 83.9° and 78.6° respectively).

Table 2 *Calculated M–L bond lengths for the Mg^{2+} and Zn^{2+} complexes of APTRA and APDAP, bound in a pentadentate manner, with one H$_2$O molecule completing the coordination sphere.*

Bond length / Å	[Mg(APDAP)]$^-$	[Mg(APTRA)]$^-$	[Zn(APDAP)]$^-$	[Zn(APTRA)]$^-$
M–N	2.233	2.336	2.366	2.382
M–OAr	2.088	2.161	2.350	2.251
M–O(CO$_2$CH$_2$O)	n/a	2.037	n/a	2.037
M–O(PO$_2$MeCH$_2$O)	1.966	n/a	1.991	n/a
M–O(CO$_2$CH$_2$N)	2.056	2.033	2.022	2.019
M–O(CO$_2$CH$_2$N)	1.971	2.028	2.020	2.013
M–O(H$_2$O)	2.093	2.135	2.302	2.258

Table 3 *Calculated L^M^L bite angles for the Mg^{2+} and Zn^{2+} complexes of APTRA and APDAP, bound in a pentadentate manner, with one H$_2$O molecule completing the coordination sphere.*

Angle / °	[Mg(APDAP)]$^-$	[Mg(APTRA)]$^-$	[Zn(APDAP)]$^-$	[Zn(APTRA)]$^-$
ArO–M–N	78.4	73.9	71.2	72.1
N–M–O$^-$	79.8	77.3	78.9	78.1
N–M–O$^-$	80.1	77.1	78.0	78.2
ArO–M–O$^-$ [(a)]	83.9	75.2	78.6	74.6

(a) O$^-$ = phosphinate oxygen for APDAP, O-carboxylate for APTRA.

(v) Discussion: the effect of structural changes in the chelate ring on metal ion selectivity

It is well established that larger metal ions will tend to suffer a larger reduction in complex stability with increasing chelate ring size than smaller cations.[1,25] Larger cations, such as Ca^{2+},

will favour the formation of 5-membered chelate rings over 6-membered, with an ideal bite angle of 69°. Smaller cations are more amenable to the formation of 6-membered chelates. A comparison between the bite angle in the O–carboxylate and O–phosphinate chelating units in APTRA and APDAP, respectively, is shown in Figure 6. A schematic of 5-membered and 6-membered chelates is also included for comparison. The increase in the ArO–M–O bite angle and the shorter M–L bond lengths found for $[Mg(APDAP)(H_2O)]^-$ suggest that the phosphinate-based APDAP ligand sets up a structure on binding to Mg^{2+} that is somewhat more like a 6-membered chelate. In 6-membered chelates, the ideal bite angle is 109.5°, significantly larger than the value of 69° for a 5-membered chelate. The larger ring chelate formed in $[Mg(APDAP)(H_2O)]^-$ may thus explain why the relative affinity for Mg^{2+} versus Ca^{2+} is increased compared to APTRA, in line with the conclusions of landmark studies by Hancock and Martell 30 years ago on 5- versus 6-membered chelates in general.[1] With regard to the specific case of phosphinates, a similar increase in affinity for smaller metal ions has been observed in phosphinate-substituted azamacrocycles, in binding studies with Cu^{2+}, Ga^{3+} and Fe^{3+}.[26]
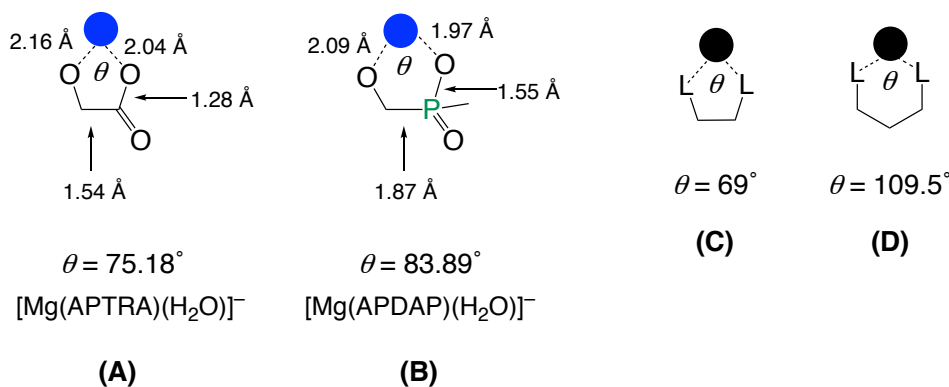

Figure 6 *Calculated ArO–M–O$^-$ bite angles in the Mg^{2+} complexes of **(A)** APTRA and **(B)** APDAP, showing the shorter M–O lengths with APDAP compared to APTRA and the longer P–O (versus C–O in APTRA) and P–C (versus C–C in APTRA). The blue circle represents the Mg^{2+} ion. Structures **(C)** and **(D)** illustrate typical 5- and 6-membered chelates formed with ligands such as ethylenediamine and trimethylenediamine respectively; the black circle represents a generic metal ion with ideal bite angles as described by Martell and Hancock.[1]*

Concluding remarks

In summary, the new, pentadentate APDAP ligand has been synthesised in a four-step sequence starting from 2-nitrophenol. Although it displays a weaker affinity towards Mg^{2+} than APTRA, the phosphinate-based ligand has a dramatically lower affinity for Ca^{2+}. The K_d values for Ca^{2+} are in the millimolar range compared to the mid-micromolar values typical of APTRA and its derivatives. The affinity for Mg^{2+} remains of an order of magnitude that renders APDAP potentially suited to biomedical applications, given that $[Mg^{2+}]$ is of the order of 1 mM in most mammalian cells. Moreover, the ligand offers high denticity, which is likely to ensure that the formation of undesirable mixed ligand species with Mg^{2+}, as occurs with β-keto acids for example, is impeded. The change in relative binding affinities of Mg^{2+} and Ca^{2+}, compared to the all-carboxylate APTRA, is probably associated with the larger chelate ring associated with the incorporation of the phosphinate unit. Future functionalization of APDAP with fluorescent groups may be anticipated to offer access to new sensors for Mg^{2+} with improved selectivity.

Experimental

(i) General

Commercially available reagents were used as received from suppliers without further purification. Solvents used were laboratory grade; anhydrous solvents were dried over the appropriate drying agent. All moisture-sensitive reactions were carried out by Schlenk-line techniques, under an inert atmosphere of either argon or nitrogen. For air sensitive reactions, solvents were degassed using the freeze-pump-thaw cycle method. Water was purified by the 'Purite$_{STILL}$plus' system with a conductivity of < 0.04 µS cm^{-1}. Thin layer chromatography was performed on neutral alumina (Merck Art 5550) or silica (Merck Art 5554) and visualized under UV irradiation (254 nm) or by staining with either iodine or potassium permanganate. Column chromatography was carried out either manually using neutral alumina or silica (Merck Silica Gel, 230 – 400 mesh) or using a Teledyne Combi-flash instrument equipped with RediSep R$_f$ silica cartridges to perform automated elution. ^1H (400 MHz) and $^{13}C\{^1H\}$ (101 MHz) and $^{31}P\{^1H\}$ (162 MHz) NMR spectra were acquired on Bruker Avance or Varian Mercury 400 NMR spectrometers. Electrospray ionisation mass spectra were acquired on a Waters TQD mass spectrometer interfaced with an Acquity UPLC system.

(ii) Optical spectroscopy; determination of pK$_a$ and metal ion affinities

UV-Vis absorption spectra were measured using a Uvikon XS spectrometer operating with LabPower software. The sample was held in a quartz cuvette with a path length of 1 cm. Spectra were recorded against pure solvent in an optically matched cuvette. pH measurements were recorded using a Jenway 3510 pH meter in combination with a Jenway 924 005 pH electrode. The pH probe was calibrated before each independent titration using commercially available buffer solutions of pH 4, 7 and 10. Samples were prepared with a background of constant ionic strength (I = 0.1 M KCl, 298 K). Aqueous solutions were titrated to acid using 0.025 M, 0.05 M and 0.1 M concentrations of HCl$_{(aq)}$. The resulting sigmoidal curve of either absorbance or fluorescence intensity vs. pH was fitted by a non-linear least squares iterative analysis by Boltzmann using Origin 8.0 software.

All metal binding studies were carried out in buffered solutions of 50 mM HEPES and 100 mM KCl maintained at pH 7.2. Stock solutions of [M^{2+}] contained the same concentration of the ligand in the cuvette, to avoid sample dilution over the course of the titration. Small aliquots of [M^{2+}] were added in each instance, with the absorbance spectrum recorded 5 minutes after each addition to ensure that the sample had equilibrated. Dissociation constants (K_d values) were calculated from the experimental data as described in the Supporting Information.

(iii) Computations

All calculations were carried out with the Gaussian 09 package.[27] The geometries were optimised at the hybrid-DFT B3LYP functional[28] with no symmetry constraints using the 6-311++G(d,p) basis set[29] for all atoms. The Gaussian default polarisation continuum model (IEFPCM)[30] was applied to all calculations using water as solvent. Frequency calculations on these optimised geometries revealed no imaginary frequencies.

**(iv) Synthetic procedures and characterisation data**

Ethyl methylphosphinate, 2
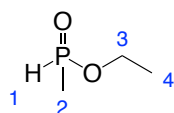
Water (264 µL, 14.7 mmol) was added to diethyl methylphosphinate **1** (2 g, 14.7 mmol) at room temperature. The colourless solution was stirred vigorously for 18 h under an inert atmosphere of argon. Reaction completion was determined by ^{31}P NMR spectroscopy. The title compound formed with one equivalent of ethanol as a by-product and was used *in situ* in subsequent steps

without any additional purification. ^{1}H NMR (400 MHz, CDCl$_3$) 7.25 (1 H, dq, J 538, 2, H[1]), 4.17 – 3.16 (2 H, m, H[3]), 1.48 (3 H, dd, J 16, 4, H[2]), 1.24 (3 H, t, J 4, H[4]); ^{13}C{^{1}H} NMR (101 MHz, CDCl$_3$) 62.4 (d, J 24, C[3]), 16.2 (d, J 24, C[4]), 14.6 (d, J 97, C[2]); ^{31}P{^{1}H} NMR (176 MHz, CDCl$_3$) + 33.4; ESI-LRMS [C$_3$H$_9$PO$_2$]$^+$ (+) m/z 109.0; ESI-HRMS calculated for [C$_3$H$_9$PO$_2$]$^+$ 109.0419 found, 109.0414.

Ethyl (hydroxymethyl)(methyl)phosphinate, 3
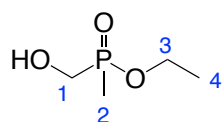
The procedure adopted was based on one developed previously for related mesylated phosphinate esters.[31] Ethyl methyl phosphinate **2** (14.7 mmol) was heated at 85°C in anhydrous THF (5 mL) for 30 min. Paraformaldehyde (707.9 mg, 23.60 mmol) was then added. The reaction mixture was heated at 75 °C under an inert atmosphere of argon and monitored by ^{31}P NMR. After 5 h the colourless solution was cooled to room temperature before the THF was removed under reduced pressure. The residue was then dissolved in CH$_2$Cl$_2$ (20 mL) before the inorganic salts were removed by filtration. The solvent was removed under reduced pressure to form a colourless oil. Purification by silica gel chromatography (gradient from 100 % CH$_2$Cl$_2$ to 90 % CH$_2$Cl$_2$/ 10 % MeOH) formed the title compound as a pale yellow oil (747 mg, 37 %). R$_f$ = 0.20 (silica, 95 % DCM; 5 % MeOH, visualisation with KMnO$_4$); ^{1}H NMR (400 MHz, CDCl$_3$) 4.13 (2 H, m, H[3]), 3.85 (2 H, m, H[1]), 3.07 (1H, br s, OH), 1.54 (3 H, d, J 12, H[2]), 1.35 (3 H, J 4, H[4]); ^{31}P{^{1}H} NMR (176 MHz, CDCl$_3$) + 52.0; ^{13}C NMR (101 MHz, CDCl$_3$) 61.1 (d, J 7, C[3]), 59.8 (d, J 110, C[1]), 17.7 (d, J 6, C[4]), 16.6 (d, J 91, C[2]); ESI-LRMS [C$_6$H$_7$[79]BrN$_2$]$^+$ (+) m/z 139.0; ESI-HRMS calculated for [C$_6$H$_7$[79]BrN$_2$]$^+$ 139.0456 found, 139.0449.

(Ethoxy(methyl)phosphoryl)methyl methanesulfonate, 4
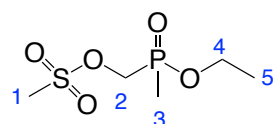
Methylsulfonyl chloride (0.65 mL, 8.4 mmol) was added to an ice cold solution of **3** (808.8 mg, 5.95 mmol) and triethylamine (1.25 mL, 8.96 mmol) in anhydrous THF (5.7 mL). The solution was warmed to room temperature and stirred for an additional 1 h under an inert atmosphere of argon. After 1 h, THF was removed under reduced pressure, the dark orange residue was re-dissolved in CH$_2$Cl$_2$ (20 mL) and washed with brine (15 mL). The organic extracts were dried

over MgSO$_4$, and the solvent was removed under reduced pressure to form an orange residue. Purification by silica gel column chromatography (gradient 100 % CH$_2$Cl$_2$ to 95 % CH$_2$Cl$_2$ / 5 % MeOH) formed the title compound as a yellow oil (1.03 g, 82 %). ^{1}H (400 MHz, CDCl$_3$) 4.46 – 4.34 (2 H, m, H^2), 4.25 – 4.11 (2 H, m, H^4), 3.15 (3 H, s, H^1), 1.63 (3 H, d, J 16, H^3), 1.39 (3 H, t, J 8, H^5); ^{31}P{^{1}H} (162 MHz, CDCl$_3$) + 43.7; ^{13}C (101 MHz, CDCl$_3$) 63.0 (d, J 106, C^2), 61.6 (d, J 7, C^4), 37.8 (s, C^1), 16.5 (d, J 6, C^5), 12.6 (d, J 100, C^3). ESI-LRMS [C$_5$H$_{13}$O$_5$PS]$^+$ (+) m/z 217.3; ESI-HRMS calculated for [C$_5$H$_{13}$O$_5$PS]$^+$ 217.0300 found, 217.0321.

Ethyl methyl((2-nitrophenoxy)methyl)phosphinate, 6
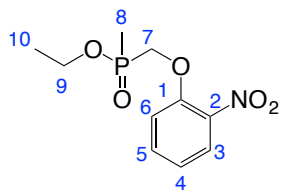
Anhydrous potassium carbonate (302.9 mg, 2.19 mmol) was added to a solution of 2-nitrophenol (98.9 mg, 0.71 mmol) and **4** (228.2 mg, 1.05 mmol) in anhydrous acetonitrile (1.2 mL). The reaction mixture was heated at 85 °C for 48 h under an inert atmosphere of argon. The pale yellow precipitate was removed by filtration and the solvent was removed under reduced pressure to form a yellow residue. Purification by silica gel column chromatography (gradient 100 % CH$_2$Cl$_2$ to 95 % CH$_2$Cl$_2$ / 5 % MeOH) formed the title product as a pale yellow oil (115.3 mg, 63 %). ^{1}H NMR (600 MHz, CDCl$_3$) 7.88 – 7 85 (1 H, m) 7.58 – 7.54 (1 H, m), 7.13 – 7.09 (2 H, m), 4.39 – 4.26 (4 H, m, H^9 and H^7), 1.69 (3 H, d, J 15, H^8), 1.33 (3 H, t, J 7, H^{10}); ^{13}C{^{1}H} (151 MHz, CDCl$_3$,) 151.8 (d, J 13, C^1), 140.1 (C^2), 134.4 (CH), 125.8 (CH), 121.9 (CH), 114.7 (C^3), 61.4 (d, J 7, C^9), 65.2 (d, J 111, C^7), 16.5 (C^9), 12.2 (C^8); ^{31}P{^{1}H} NMR (242 MHz, CDCl$_3$) + 48.5; ESI-LRMS [C$_{10}$H$_{14}$NO$_5$P]$^+$ (+) m/z 260.1; ESI-HRMS calculated for [C$_{10}$H$_{14}$NO$_5$P]$^+$ 260.0701 found 260.0699.

Ethyl ((2-aminophenoxy)methyl)(methyl)phosphinate, 7
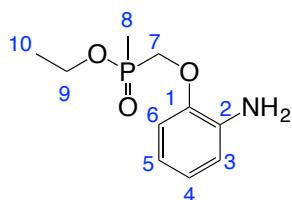
Compound **6** (118.1 mg, 0.46 mmol) was dissolved in ethanol (20 mL). Palladium on charcoal (10 wt. %, 51.6 mg, 0.03 mmol) was added and the reaction mixture was stirred at room temperature for 2 h under an atmosphere of hydrogen. After this time, the reaction mixture was filtered through a celite plug. The solvent was removed under reduced pressure to form a pale yellow oil (104 mg, 96 %). Compound **7** was used in subsequent steps without any additional

purification. ^{1}H NMR (600 MHz, CDCl$_3$) 6.86 – 6.82 (2 H, m, H^3, H^4, H^5 or H^6), 6.74 – 6.70 (2 H, m, H^3, H^4, H^5 or H^6), 4.29 – 4.07 (4 H, m, H^7 and H^9), 1.64 (3 H, d, J 14.6, H^8), 1.34 (3 H, t, J 7, H^{10}); ^{31}P{^{1}H} NMR (162 MHz, CDCl$_3$) + 47.4; ^{13}C{^{1}H} (151 MHz, CDCl$_3$) 146.3 (d, J 11.9, C^1), 136.4 (C^2), 122.8 (C^3, C^4, C^5 or C^6), 118.5 (C^3, C^4, C^5 or C^6), 115.7 (C^3, C^4, C^5 or C^6), 112.2 (C^3, C^4, C^5 or C^6), 64.6 (d, J 111, C^7), 61.0 (d, J 7, C^9), 16.6 (s, C^{10}), 12.6 (d, J 98, C^8); ESI-LRMS [C$_{10}$H$_{16}$NO$_3$P]$^+$ (+) m/z 230.6; ESI-HRMS calculated for [C$_{10}$H$_{16}$NO$_3$P]$^+$ 230.0946 found 230.0949.

Diethyl 2,2'-((2-((ethoxy(methyl)phosphoryl)methoxy)phenyl) azanediyl) diacetate, 8
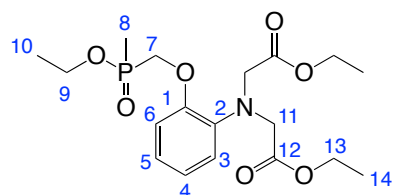
N,N-Diisopropylamine (410 µL, 2.36 mmol) and ethyl bromoacetate (158 µL, 1.42 mmol) were added to a solution of **7** (107.5 mg, 0.46 mmol) and sodium iodide (125.6 mg, 0.97 mmol) in anhydrous acetonitrile. The reaction was heated for 2 d at 85 ^{o}C under an inert atmosphere of argon before the addition of further N,N-diisopropylamine (120 µL, 0.69 mmol) and ethyl bromoacetate (50 µL, 0.45 mmol). The reaction mixture was stirred at 85 ^{o}C for a further 2 d, before being cooled and diluted with ethyl acetate (10 mL). Inorganic impurities were removed by filtration before the organic filtrate was washed with water (10 mL) and brine (10 mL). Organic extracts were combined and dried over MgSO$_4$, and the solvent was removed under reduced pressure to form a pale brown residue. Purification by silica gel column chromatography (gradient 1:1 hexane / ethyl acetate to 100 % ethyl acetate) formed the title compound as a pale brown oil (97.3 mg, 53 %). ^{1}H NMR (700 MHz, CDCl$_3$) 6.95 – 6.93 (3 H, m, H^3, H^4, H^5 or H^6), 6.90 – 6.88 (1 H, m, H^3, H^4, H^5 or H^6), 4.32 – 4.05 (14 H, m, H^7, H^9, H^{11} and H^{13}), 1.66 (3 H, d, J 15, H^8), 1.33 (3 H, t, J 7, H^{10}), 1.23 (6 H, t, J 7, H^{14}); ^{31}P{^{1}H} NMR (283 MHz, CDCl$_3$) + 48.3; ^{13}C{^{1}H} NMR (176 MHz, CDCl$_3$,) 170.9 (s, C^{12}), 150.9 (d, J 11, C^1), 139.4 (s, C^2), 122.9 (s, C^3, C^4, C^5 or C^6), 122.7 (s, C^3, C^4, C^5 or C^6), 120.8 (s, C^3, C^4, C^5 or C^6), 117.4 (s, C^3, C^4, C^5 or C^6), 64.8 (d, J 6, C^7 or C^9), 60.9 (d, J 7, C^7 or C^9), 60.7 (s, C^{11} or C^{13}), 53.2 (s, C^{11} or C^{13}), 16.5 (d, J 6, C^{10}), 14.2 (s, C^{14}), 12.5 (d, J 97, C^8); ESI-LRMS [C$_{18}$H$_{29}$NO$_7$P]$^+$ (+) m/z 402.6; ESI-HRMS calculated for [C$_{18}$H$_{29}$NO$_7$P]$^+$ 402.1682 found 402.1694; Reverse phase HPLC (0 % - 100 % - 0% CH$_3$CN in ammonium bicarbonate buffer (25 mM), t_R = 9.6 min).

2,2'-((2-((Hydroxy(methyl)phosphoryl)methoxy)phenyl)azanediyl) diacetic acid, APDAP
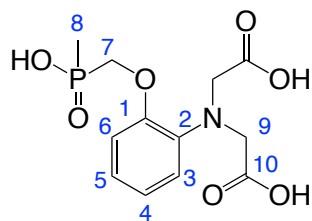
The tris-ester **8** (82.6 mg, 0.21 mmol) was dissolved in CD$_3$OD (4 mL) and NaOD (0.4 M in D$_2$O, 1.4 mL). The pale yellow solution was stirred under an inert atmosphere of argon at room temperature for 20 h. Hydrolysis of the ethyl esters was monitored by ^{1}H NMR spectrometry, ^{31}P NMR spectrometry and ESI-LRMS. The solution was lyophilized to form the title compound as an off-white solid in almost quantitative yield (62 mg, 93 %). ^{1}H NMR (600 MHz, D$_2$O) 6.95 (1 H, dd, J 1.8, 8, H^6), 6.83 (2 H, m, H^4 and H^5), 6.78 (1 H, br m, H^3), 3.93 (2 H, d, J 9, H^7), 3.71 (4 H, s, H^9), 1.29 (3 H, d, J 14, H^8); ^{31}P{^{1}H} NMR (283 MHz, D$_2$O) + 36.54; ^{13}C{^{1}H} NMR (176 MHz, D$_2$O) 179.1 (C^{10}), 150.6 (C^1) 139.4 (C^2), 121.6 (C^4 or C^5), 118.5 (C^4 or C^5), 118.1 (C^3), 113.4 (C^6), 56.5 (C^9), 14.2 (d, J 95, C^8); Reverse phase HPLC (0 % - 100 % - 0% CH$_3$CN in ammonium bicarbonate buffer (25 mM), t_R = 1.2 min).

Acknowledgements

References

1. R. D. Hancock and A. E. Martell, *Chem. Rev.*, 1989, **89**, 1875.
2. D. L. Wright, J. H. Holloway and C. N. Reilley, Anal. Chem., 1965, **37**, 884.
3. J. R. Hart, *J. Chem. Educ.*, 1984, **61**, 1060; *Idem., ibid.*, 1985, **62**, 75; O. J. Grundler, A. T. M. van der Steen and J. Wilmot, in "Overview of the European Risk Assessment on EDTA", ACS Symposium Series, 2005, chpt. 21.
4. R. Y. Tsien, *Biochemistry*, 1980, **19**, 2396.
5. R. Y. Tsien in "Fluorescent Chemosensors for Ion and Molecule Recognition", Ed. A. W. Czarnik, American Chemical Society: Washington DC, 1993, chpt. 9.
6. B. Raju, E. Murphy, L. A. Levy, R. D. Hall and R. E. London, *Am. J. Physiol.*, 1989, **256**, C540.
7. B. Morelle, J. M. Salmon, J. Vigo and P. Viallet, *Anal. Biochem.*, 1994, **218**, 170.
8. *For example:* C. A. Reid, R. Fabian-Fine and A. Fine, *J. Neurosci.*, 2001, **21**, 2206.

9. L. A. Levy, E. Murphy, B. Raju and R. E. London, *Biochemistry*, 1988, **27**, 4041; B. Raju, E. Murphy, L. A. Levy, R. D. Hall and R. E. London, *Am. J. Physiol.*, 1989, **256**, 540; P. A. Otten, R. E. London and L. A. Levy. *Bioconjugate. Chem.*, 2001, **12**, 7.

10. R. A. Bissell, A. P. de Silva, H. Q. N. Gunaratne, P. L. M. Lynch, G. E. M. Maguire, C. P. McCoy, K. R. A. S. Sandanayake, *Top. Curr. Chem.*, 1993, **168**, 223; A. P. de Silva, H. Q. N. Gunaratne and G. E. M. Maguire, *J. Chem. Soc., Chem. Commun.*, 1994, 1213.

11. M. S. Afzal, J-P. Pitteloud and D. Buccella, *Chem. Commun.*, 2014, **50**, 11358; Zhang, J. J. Gruskos, M. S. Afzal and D. Buccella, *Chem. Sci.*, 2015, **6**, 6841; Q. Lin, J. J. Gruskos and D. Buccella, *Org. Biomol. Chem.*, 2016, **14**, 11381.

12. P. A. Otten, R. E. London and L. A. Levy. *Bioconjugate. Chem.*, 2001, **12**, 203.

13. T. Fujii, Y. Shindo, K. Hotta, D. Citterio, S.Nishiyama, K. Suzuki and K. Oka, *J. Am. Chem. Soc.*, 2014, **136**, 2374.

14. S. C. Schwartz, B. Pinto-Pacheco, J-P. Pitteloud and D. Buccella, *Inorg. Chem.*, 2014, **53**, 3204.

15. S. L. Volpe, *Adv. Nutr.*, 2013, **4**, 378S.

16. A. M. P. Romani, *Arch. Biochem. Biophys.*, 2007, **458**, 90.

17. C. B. Black, H. W. Huang, J. A. Cowan, *Coord. Chem. Rev.*, 1994, **135**, 165; J. Sponer, J. Leszczynski and P. Hobza, *Biopolymers*, 2001, **61**, 3.

18. M. Tilmann and F. Wolf, *Curr. Opin. Pediatr.*, 2017, **29**, 187.

19. L. M. Resnick, *Am. J. Hypertens.*, 1993, **6**, 123S.

20. J. L. Glick, *Med. Hypotheses*, 1990, **31**, 211; N. Veronese, A. Zurlo, M. Solmi, C. Luchini, C. Trevisan, G. Bano, E. Manzato, G. Sergi and R. Rylander, *Am. J. Alzheimers. Dis. Other. Demen.*, 2016, **31**, 208.

21. A. Tin and M. E. Grams. *Kidney. Int.*, 2015, **87**, 820.

22. M. Brady, S. D. Piombo, C. Hu and D. Bucella, *Dalton Trans.*, 2016, **45**, 12458.

23. M. Booy and T. W. Swaddle, *Can. J. Chem.*, 1977, **55**, 1762.

24. O. Reaney, T. Gunnlaugsson and D. Parker, *J. Chem. Soc., Perkin Trans. 2*, 2000, 1819.

25. R. D. Hancock, *J. Chem. Educ.*, 1992, **69**, 615.

26. E. Cole, R. C. B. Copley, J. A. K. Howard, D. Parker, G. Ferguson, J. F. Gallagher, B. Kaitner, A. Harrison and L. Royle, *J. Chem. Soc., Dalton Trans.*, 1994, 1619.

27. M. J. Frisch, G. W. Trucks, H. B. Schlegel, G. E. Scuseria, M. A. Robb, J. R. Cheeseman, G. Scalmani, V. Barone, B. Mennucci, G. A. Petersson, H. Nakatsuji, M. Caricato, X. Li, H. P. Hratchian, A. F. Izmaylov, J. Bloino, G. Zheng, J. L. Sonnenberg, M. Hada, M. Ehara, K. Toyota, R. Fukuda, J. Hasegawa, M. Ishida, T. Nakajima, Y. Honda, O. Kitao, H. Nakai, T.

Vreven, Jr., J. A. Montgomery, J. E. Peralta, F. Ogliaro, M. Bearpark, J. J. Heyd, E. Brothers, K. N. Kudin, V. N. Staroverov, R. Kobayashi, J. Normand, K. Raghavachari, A. Rendell, J. C. Burant, S. S. Iyengar, J. Tomasi, M. Cossi, N. Rega, J. M. Millam, M. Klene, J. E. Knox, J. B. Cross, V. Bakken, C. Adamo, J. Jaramillo, R. Gomperts, R. E. Stratmann, O. Yazyev, A. J. Austin, R. Cammi, C. Pomelli, J. W. Ochterski, R. L. Martin, K. Morokuma, V. G. Zakrzewski, G. A. Voth, P. Salvador, J. J. Dannenberg, S. Dapprich, A. D. Daniels, O. Farkas, J. B. Foresman, J. V. Ortiz, J. Cioslowski, D. J. Fox, *Gaussian 09*, Revision A.02, Gaussian, Inc., Wallingford CT, 2009.

28. A. D. Becke, *J. Chem. Phys.,* 1993, **98**, 5648; C. Lee, W. Yang and R. G. Parr, *Phys. Rev. B.,* 1988, **37**, 785.

29. G. A. Petersson and M. A. Al-Laham, *J. Chem. Phys.* 1991, **94**, 6081; G. A. Petersson, A. Bennett, T. G. Tensfeldt, M. A. Al-Laham, W. A. Shirley and J. Mantzaris, *J. Chem. Phys.,* 1988, **89**, 2193; M. J. Frisch, J. A. Pople and J. S. Binkley, *J. Chem. Phys.,* 1984, **80**, 3265; A. D. McLean and G. S. Chandler*, J. Chem. Phys.* 1980, *72*, 5639.

30. J. Tomasi, B. Mennucci and E. Cancès, *J. Mol. Struct. (Theochem)*, 1999, **464**, 211.

31. C. J. Broan, E. Cole, K. J. Jankowski, D. Parker, K. Pulukkody, B. A. Boyce, N. R. A. Beeley, K. Millar and A. T. Millican, *Synthesis*, 1992, 63.